(22) Inoue, Y.; Fukutomi, T.; Chûjô, R. *Polym. J. (Tokyo)* **1983**, *15*, 103.
(23) Zekhnini, Z. Thèse de 3e cycle, Université Louis Pasteur, Strasbourg, 1985.
(24) Moens, J.; Smets, G.; *J. Polym. Sci.* **1957**, *23*, 931.
(25) Mayo, F. R.; Lewis, F. M. *J. Am. Chem. Soc.* **1944**, *66*, 1594.
(26) Reichert, K. H.; Baade, W. *Angew. Makromol. Chem.* **1984**, *123/124*, 361.
(27) Halverson, F.; Lancaster, J. E.; O'Connor, M. N. *Macromolecules* **1985**, *18*, 1139.
(28) Auvray, L.; Cotton, J. P.; Ober, R.; Taupin, C. *J. Phys.* **1984**, *45*, 913.

A ^{13}C NMR Method for Determining the Partitioning of End Groups and Side Branches between the Crystalline and Noncrystalline Regions in Polyethylene

D. L. VanderHart* and E. Pérez

Polymers Division, National Bureau of Standards, Gaithersburg, Maryland 20899.
Received December 30, 1985

ABSTRACT: An ethylene–1-butene linear copolymer (E/B) is shown to give rise to a solid-state ^{13}C spectrum which, when taken with proton–carbon cross polarization (CP), magic-angle spinning, and high-power proton decoupling, contains resolvable resonances from vinyl and methyl end groups as well as ethyl side branches. The signal-to-noise generated after 12–20 h of transient accumulation is sufficient to identify signals of the order of 2 carbons per 10 000 backbone carbons. In contrast to the backbone methylene resonance, which shows shifted, separable signals arising from the crystalline and noncrystalline regions, these weak "defect" resonances show corresponding shifts too small to be definitive. Therefore, the problem of determining the partitioning of defects between the crystalline and noncrystalline regions of polyethylene must be approached indirectly. The method for identifying the morphological origin of defect signals is based on the concept that ^{13}C CP signals are proportional to the local spin polarization levels, which, in turn, are kept quite uniform over distances of nearest neighbors because of proton spin diffusion. Thus, defect signal intensities are argued to be proportional to backbone signal intensities within a given morphological region. By isolating the backbone resonances corresponding to the pure crystalline and noncrystalline components, one thereby isolates the defect resonances. The determination of these pure component line shapes was accomplished by changing the preparation of the proton spin states prior to CP in ways which changed the mixture of crystalline and noncrystalline components in the resulting spectra. Since it is not obvious that the CP efficiency of the backbone carbons and the defect carbons in a given region should be the same, the consistency of the CP intensities with intensities expected based on solution ^{13}C NMR results was probed. In this initial study of the E/B slowly cooled from the melt, the vinyl and methyl end-group carbon resonances were found to have enhancement factors very similar to those of the backbone methylene carbons. The crystalline region, having a mass fraction of 0.76, contained 57% of the methyls and 46% of the vinyls. The fraction of crystalline vinyls in this study is substantially larger than that found in solution-grown crystals in other studies. In contrast, the ethyl-branch carbons were not so well-behaved; i.e., their total intensity was not fully accounted for. Taking account of the missing intensity and the limits of sensitivity, we argue that no more than 20% of the ethyl branches resides in the crystal. On the other hand, there was no direct evidence that any crystalline ethyl branches exist. Studies of this question and others will appear in forthcoming papers.

I. Introduction

^{13}C studies of polyethylene (PE) in solution have yielded a wealth of information about the amount and nature of short-chain branches.[1-4] Long-chain branches are also observed;[1,3-5] moreover, the methyl and α- and β-methylene carbons of saturated chain ends as well as allylic methylene carbons adjacent to terminal vinyl groups are also easily resolved.

Solid-state ^{13}C NMR employing high-power proton decoupling[6,7] and magic-angle spinning[8-11] also yields high-resolution spectra although line widths are typically 10–100 times broader than in solution.[12-15] In contrast to solution spectra, the solid-state spectra may show evidence of heterogeneous environments such as the coexistence of multiple unit cells[16] or the coexistence of crystalline (ordered) and noncrystalline (disordered) regions.[17] The latter consideration dominates the interpretation of the ^{13}C PE spectrum, which, at 50 MHz, typically consists of a sharp crystalline resonance centered at 32.9 ppm[18] and a broader noncrystalline shoulder centered at 31.1 ppm. Since chemical shifts for saturated hydrocarbons in the solid are usually within a few ppm of those found in solution,[19] it is clear from the solution work that several end-group or side-branch resonances (referred to collectively as defect resonances) should be resolvable from the main backbone resonances. In fact, in crystalline *n*-alkanes, the methyl, the α-methylenes, and the β-methylenes are all distinct from the interior methylene resonances.[19] In polyethylene, fewer resonances than in the *n*-alkanes will be distinguishable due to both the much weaker intensity of the defect resonances and the broad, rather intense, noncrystalline resonance. Nevertheless, weak resonances with chemical shifts outside the range of 26–38 ppm are expected to be visible. This includes all methyls, α-methylenes (marginal), methine branch carbons (marginal), and vinyl carbons (terminal and interior). Therefore, the observation of these resonances is possible, in principle. The only questions are those of sensitivity and cross-polarization (CP) efficiency.

The advantage of the solid-state ^{13}C measurements compared with liquid-state studies, therefore, is that the solid-state morphology is present. In this paper we do not seek to argue for the superiority of the solid-state approach over liquid-state methods in determining defect concentration. Rather, we seek to probe the *location* of the defect resonances, i.e., how the side groups and end groups are

0024-9297/86/2219-1902$01.50/0

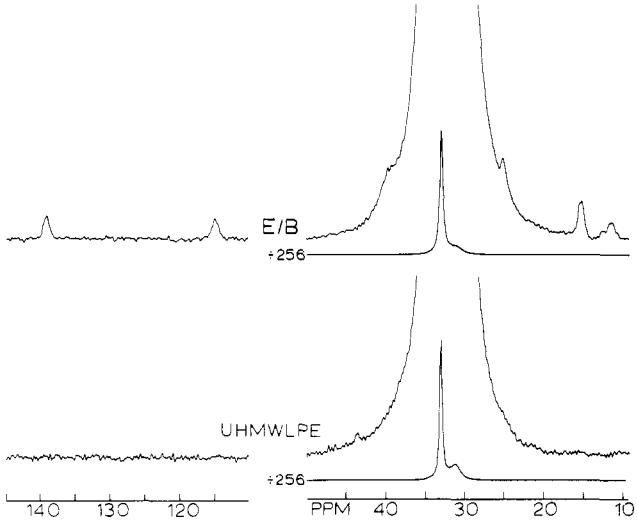

Figure 1. 50-MHz CP–MAS ^{13}C spectra of the vinyl and aliphatic regions of the E/B (upper) and UHMWLPE (lower) samples. CP times of 1 ms were used; the E/B and UHMWLPE spectra result from averaging 11 000 and 5000 transients, respectively. Spectra are normalized to the same total intensity. Resonance assignments for the end-group and side-branch carbons are discussed in the text. The backbone resonances are shown with an amplification factor 256 times lower than for the remaining spectral profiles.

partitioned between the crystalline and noncrystalline phases of polyethylene.

It is emphasized that a *melt*-crystallized sample is used in this preliminary study. Previous studies on the partitioning of vinyl end groups have used single-crystal preparations in order to ensure access of a reactive chemical, either ozone[20,21] or bromine.[22,23] In both the latter studies it was concluded that 85–98% of the vinyl end groups are accessible for reaction and assumed, thereby, to be rejected by the crystal. The results of this study show melt crystallization to be much less discriminating toward vinyl ends.

II. Basis for the Experiment

The first criterion for proceeding is to establish that one can observe the expected resonances from the defects and that these resonances are indeed due to the defects and not, for example, chain conformation.[24,25] In Figure 1 the CP–MAS spectrum of the ethylene–1-butene linear copolymer (E/B), the material upon which most of the work reported herein was done, is compared with a spectrum of an ultrahigh molecular weight linear polyethylene (UHMWLPE). Under amplification, the UHMWLPE spectrum only shows a very small peak around 43 ppm in addition to the usual resonances at 32.9 and 31.1 ppm. A very small amount of monoclinic crystalline material is also barely discernible at 34.3 ppm in the unamplified spectrum. The 43 ppm peak is probably due to methylene carbons adjacent to a carbonyl,[3,26] most of which were probably formed when the UHMWLPE plug was molded at 200 °C. No evidence of any tight chain folds is to be found upfield from the noncrystalline resonance line.[25] On the other hand, the E/B spectrum is rich in weak resonances. Resonances at 11.3, 15, 25, 40, 115, and 139 ppm can be assigned to the $1B_2$, 1s, 2s, brB_2, 1u, and 2u carbons of the following drawing, in analogy to solution results.[1-5]

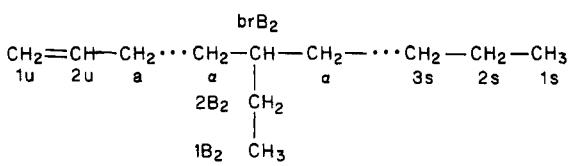

Other portions of the spectrum, not shown, only contain spinning sidebands of the crystalline carbons. After 5000–10 000 transients are signal-averaged in a normal CP experiment, weak resonances representing carbon fractions of the order of 2×10^{-4} can be discerned, and integrals accurate to $\pm 10^{-4}$ may be established, provided the base line is well-defined on both sides of the line, as it is for the vinyl resonances. In Figure 1, the methine resonance at 40 ppm and the 2s resonance at 25 ppm are visible but difficult to integrate because of their overlap with the wings of the backbone resonances. The methyls, on the other hand, are well resolved, with the ethyl methyl quite distinct from the end methyl of a linear chain. In any case, in this material, at least one resolvable resonance can be identified with each of the following types of defects: vinyl ends, saturated ends, and ethyl branches. We turn now to the question of separating these defect resonances into contributions from the different morphological regions.

In order to define the location (the crystalline or noncrystalline region) of a defect, one must make a few assumptions, each of which is, in our opinion, reasonable. First, the backbone methylene resonance profile may be used to separate the contribution from crystalline and noncrystalline carbons; crystalline carbons are those which resonate in the narrow band at 32.9 ppm. Second, polyethylene will be regarded as a simple two-phase system. Third, ^{13}C signals obtained after ^{13}C–^{1}H cross polarization (CP) for a given time are proportional to the polarization level (spin temperature) of the nearby protons. Fourth, during the CP period end-group or side-branch protons will have polarization levels which are very close to those of their immediately neighboring backbone methylene protons. This latter postulate is made on the basis of efficient proton spin diffusion in solids. It follows from this postulate that even though the motions of given end groups or side branches may be qualitatively different from those of their neighboring backbone methylenes, ^{13}C CP signals from those defects will be proportional to the intensity of the neighboring backbone resonances. (Mobility-based differences in CP enhancement factors between defect and backbone resonances are allowed.) Basically, this fourth postulate says that no defects give rise to truly liquid-like resonances; i.e., the protons involved in all defects maintain a reasonable degree (at least a few kilohertz) of dipolar coupling to the backbone protons. Fifth, it will be assumed that the defects are evenly distributed within each phase.

While the above postulates are expected to be true for most sites in polyethylene, we do not wish to argue that polyethylene (PE) is strictly a two-phase system without any interfaces,[27] nor do we deny that in some samples one observes a narrow component[28] in the proton spectrum whose intensity is usually less than a couple of percent and whose line width is the order of 1–3 kHz for PE samples with molecular weight less than 10^5. Thus, since the approach taken here is somewhat simplifying, the results will be something less than rigorously quantitative. Where possible, data will be included bearing on the validity of these postulates, including postulate five concerning the uniform distribution of defects.

Because of the distinct possibility that defect carbons, particularly those in the noncrystalline region, will have CP efficiencies different from those of the backbone carbons, it was deemed necessary to have independent data on M_n values and defect concentrations. Most of this characterization was obtained by solution ^{13}C NMR. The defect intensities in the CP spectra could then be compared with the backbone intensities in order to see if all

of the expected defect intensity was accounted for. This accounting is made more difficult, however, because of the different CP behaviors of the crystalline and noncrystalline backbone carbon resonances. The CP enhancement factor, $\epsilon_{NC}(t)$, which is equal to the ratio of the noncrystalline signal (after a CP period of duration t) to the signal from the equilibrium Boltzmann population of those carbons, is always less than the corresponding crystalline CP enhancement factor, $\epsilon_C(t)$, no matter what value of t is chosen. The reason for this is that the proton rotating-frame relaxation time, $T_{1\rho}^H$, is shorter in the noncrystalline region and the time constant for CP, T_{CH}, is longer than the corresponding values in the crystal. Typical values[16] for t = 1 ms are ϵ_{NC} = 2–3 and ϵ_C = 3.5–3.7. Since $5T_{CH} < 1$ ms and since 1 ms $\ll T_{1\rho}^H$ for the crystalline backbone chains, ϵ_C does not vary appreciably from sample to sample. However, since the noncrystalline chain mobility and fraction are very sample dependent, ϵ_{NC} must be measured for each sample in order to determine the true crystallinity and to relate the defect resonance intensities to their true concentrations. A reasonable assumption when one is trying to account for total defect intensity is that the enhancement factor ϵ_C^d for any defects in the crystalline region is approximately the same as ϵ_C. This is rationalized on the basis of the strong dipolar fields and the strong resulting spin diffusion and short T_{CH} due to the rigid backbone chains which surround the defect in the lattice. Moreover, the large spin heat capacity of the backbone protons relative to the defect protons will determine the proton spin polarization of the defect protons even though, locally, the defect may show more mobility than the backbone.

The final consideration in this method is the procedure by which the crystalline and noncrystalline resonances are isolated. The method is quite simple. One generates CP spectra using different preparations of the proton spins prior to the CP period (see Experimental Section). In this manner spectra representing different mixtures of crystalline and noncrystalline resonances can be observed. Appropriate linear combinations of each pair of such spectra will yield either a "pure crystalline" or a "pure noncrystalline" spectrum for the backbone carbons. From the five assumptions discussed previously, these same pure spectra also represent the pure spectra of the defects in the sense that no defect resonances of noncrystalline origin appear in the crystalline spectra and vice versa. However, the intensities of the defect resonances are faithfully reproduced only if the ϵ values are the same for the backbone and defect resonances in each phase. In this paper, three original spectra were utilized. Isolation of the "pure" spectra then becomes an overdetermined problem so that the two sets of three individual "pure" spectra can be compared within each set as a check for the self-consistency of the method.

III. Experimental Section

A. NMR Considerations. The ^{13}C spectra were recorded at 50.3 MHz on a Bruker CXP200 spectrometer[29] equipped with a CP–MAS probe manufactured by Doty Scientific, Inc.[29] The rotors consist of 7-mm-o.d. sapphire cylinders equipped with poly(trifluorochloroethylene) end caps; the stator is made of aluminum oxide. Therefore, background signals do not exist in CP spectra, which utilize the alternating spin temperature inversion with alternate addition and subtraction of data.[30]

In recording these spectra, one must take care to avoid the usual resonances from spinning sidebands and quadrature images. Therefore, the radiofrequency carrier was placed at about 5 ppm and spinning speeds were set at 2800–3500 Hz so as to avoid overlap of the sidebands with the regions of interest. There was one rather annoying feature about the probe, however. A dispersion-like signal shifted by about 26–27 ppm on either side of the strong crystalline resonance line was always visible in the CP spectra. This signal was of the order of 2×10^{-3} times the central line intensity and was probably due to a mechanical response of the probe to the turn-off of the carbon radio frequency. Signal averaging had no effect on this signal. Fortunately this spurious signal lay outside of our region of interest; however, its presence limited the amount of well-defined base line on the high-field side of the spectrum. Therefore, the uncertainty in the integration of the ethyl methyl region at 11.3 ppm is greater than it would be in the absence of this spurious signal.

The pulse sequences used to generate the three spectra which were utilized for isolating the pure crystalline and pure noncrystalline spectra are designated "CP", "SL20+CP", and "DE5+CP". Each sequence, prior to ^{13}C signal observation, involves a 1-ms CP period. The sequences only differ in the preparation of the protons prior to CP. For the CP sequence, only the usual 90° preparation pulse[7] is used. For the SL20+CP sequence, there is a 20-ms spin-locking period, and for the DE5+CP sequence, there is an initial 90° pulse followed by five, phase-shifted 90° pulses applied at odd multiples of τ following the initial 90° pulse. This sequence produces a train of five dipolar echoes.[31-33] CP begins in the center of the final echo; the value chosen for τ was 12 μs. In the CP spectrum all of the carbons have comparable intensities even though the ϵ_{NC} values are smaller than the ϵ_C values. In the SL20+CP sequence, signals from the crystalline regions where $T_{1\rho}^H$ is longer are enhanced although proton spin diffusion prevents each phase from behaving as an isolated spin system. Finally, in the DE5+CP experiment, carbons near the protons with the narrower line widths are enhanced. During MAS, the angular part of the secular proton–proton dipolar Hamiltonian becomes time dependent and periodic. Thus, the dipolar echo sequence, which depends for its success[31] on the time independence of the dipolar interaction, as well as a choice of τ which is less than T_2^H is doubly inefficient for the crystalline protons. The result is that the proton magnetization associated with the more mobile noncrystalline chains survives, thereby yielding a noncrystalline-rich spectrum. Given the usual range of crystallinity in PE of 0.6–0.8, it is clear that a sequence like the DE5+CP will produce a much weaker signal than the other two sequences, especially when one realizes that only about 50% of the noncrystalline signal is observed. Thus, while 5000–10 000 transients are very adequate for collecting spectra using the CP and SL20+CP sequences, 25 000–50 000 transients must be accumulated in the DE5+CP experiment and even then the signal-to-noise level in the latter spectrum is poorer.

The pulse sequence used to measure ϵ_{NC} is designated by (90°–5 s). The actual sequence, however, included a 3-s waiting period following signal observation to allow the protons to approximate equilibrium. After this period two 90° carbon pulses separated by 1 ms were applied in order to saturate the ^{13}C polarization. Following those saturation pulses, there was a 5-s delay and then signal observation. This method ensured that there was no contribution from transient Overhauser enhancements[34] since the proton longitudinal relaxation time, T_1^H, was less than 1 s. After 5-s delay, the noncrystalline signals are at full strength since the noncrystalline longitudinal relaxation time, T_1^C, for the backbone carbons is less than 0.5 s.[17,35] A few experiments using delays longer than 5 s indicated that the methyl resonances were also at their equilibrium levels for the entire population of methyls. Therefore, this experiment provided the information necessary for determing ϵ_{NC}, which, in turn, gave a value for the true crystallinity, f_c, because ϵ_C was assumed to be 3.5. In addition, this experiment, when combined with the true crystallinity, yielded much needed information on total methyl concentration.

The rotating radio-frequency field strengths for both carbons and protons were approximately 70 kHz. A dwell time of 25 μs was used with an 8K Fourier transform. In order to avoid ringing (and apparent peaks) due to any truncation, acquisitions for the CP and SL20+CP sequences were set at 76 ms. Since the DE5+CP and (90°–5 s) sequences produced principally broader noncrystalline resonances, only a 38-ms decoupling period was employed. The delay time between experiments was chosen to be 7, 8, and 3 s, respectively, in order to reduce probe heating. A decaying trapezoidal apodization was applied to the free induction decays at the 50-ms point in the CP and SL20+CP ex-

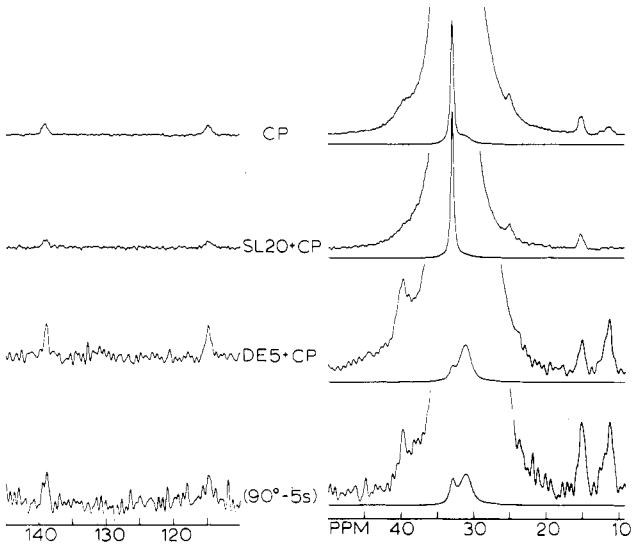

Figure 2. ^{13}C MAS E/B spectra resulting from the four experiments discussed in the text. The upper three spectra are CP spectra having differing relative contributions from crystalline and noncrystalline signals. All spectra are normalized to the same total intensity so that defect resonances (amplified times 128 with respect to the backbone resonances profiles) may be compared on the basis of concentrations. From top to bottom these spectra represent the accumulation of 11 000, 11 000, 30 000, and 7000 transients. Note the poorer signal-to-noise level of the DE5+CP and (90°–5 s) experiments compared to the other two.

periments and at the 32.5-ms points in the DE5+CP and (90°–5 s) experiments. Typical crystalline line widths in the CP and SL20+CP experiments were 0.4 ppm.

B. Samples. The UHMWLPE sample was formed from a Hifax series polyethylene manufactured by Hercules. Molecular weight exceeds 2×10^6. The sample was machined into a 6-mm-o.d. cylinder using a 12-mm-o.d. cylindrical plug which had been compression molded at 200 °C.

The E/B (BHV 5003, lot 01-5-1810) was made by Phillips Petroleum and was obtained from J. Randall, who also gave us the sample characterization information as follows. By ^{13}C NMR: M_n = 13 200; defect concentrations per 1000 backbone carbons: methyl ends, 1.13; vinyl ends, 0.99; ethyl branches, 2.7. By GPC: M_n = 11 900, M_w = 220 000, so this sample is very polydisperse. Characterization by ^{13}C NMR was also repeated at 100 MHz in our laboratory. Our analysis gave very similar defect concentrations per 1000 backbone carbons: methyl ends, 1.25 ± 0.10; vinyl ends, 1.03 ± 0.10; ethyl branches, 2.6 ± 0.15. The end-group concentrations yield M_n = 12 300.

The particular E/B sample used in this study was made by melting the as-received pellets at 155 °C for 13 min in a cylindrical die and slowly cooling the sample over 30 min to 90 °C while applying mild pressure to eliminate voids during crystallization. The resulting cylinder was then machined to the correct cylinder dimensions for insertion in the rotor.

IV. Results

Spectra resulting from the CP, SL20+CP, DE5+CP, and (90°–5 s) experiments are shown in Figure 2. Two levels of amplification are shown: ×1 and ×128 for the aliphatic region while only the ×128 scale is used in the vinyl region. It is very important to note that each spectrum shown is normalized to the same total intensity. Already by inspection of the crystalline-rich SL20+CP spectrum and the noncrystalline-rich DE5+CP spectrum, it is apparent that, expressed as *concentration*, the end-group resonances, both vinyl and methyl, prefer to be in the noncrystalline region. As for the ethyl branches, they seem to be found exclusively in the noncrystalline phase, judging by both the 11 and 40 ppm regions. The stronger end-methyl intensity (15 ppm) in the (90°–5 s) vs. the DE5+CP experiment is rationalized at this point by the recognition

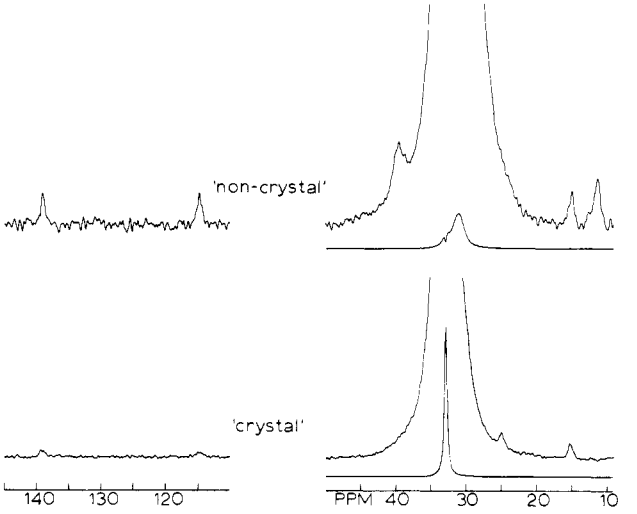

Figure 3. ^{13}C MAS spectra corresponding to the pure noncrystalline (upper) and pure crystalline (lower) regions of the E/B sample. These spectra have been obtained from the three CP spectra of Figure 2 by the method outlined in the text. Spectra are normalized to the same total intensity. The amplification contrast factor is 128.

Table I
Relative Intensities and Line-Shape Analyses for the Various Spectra

expt	area[a] per scan	crystal area[a,b]	noncrystal area[a,b]	app crystal content
CP	9.51	7.88	1.63	0.83
SL20+CP	5.92	5.62	0.30	0.95
DE5+CP	0.94	0.07	0.87	0.07
(90°–5 s)	0.98	0.27	0.71	0.28

[a] In arbitrary units. [b] Based on the "pure" component line shapes.

that all end methyls are included in the former spectrum while mostly noncrystalline end methyls appear in the latter spectrum.

The "pure crystalline" and "pure noncrystalline" spectra were determined in the manner described earlier and are shown in Figure 3. If the CP, SL20+CP, and DE5+CP spectra are designated respectively as A, B, and C, then the pure crystalline spectrum is generated by averaging the renormalized spectra obtained with the following linear combinations: B – 0.271A; B – 0.054C; and A – 0.188C. Likewise, the linear combinations used to generate the pure noncrystalline spectrum were A – 0.817B, C – 0.058B, and C – 0.073A.

The "pure" spectra of Figure 3 were used to decompose the spectra of Figure 2 into their respective contributions. These are listed in Table I. From these data one can see that the DE5+CP experiment possesses the worst intrinsic signal-to-noise of the three CP experiments. Moreover, this signal-to-noise is comparable to that of the (90°–5 s) experiment. Also, from Table I, the value for ϵ_{NC} is determined to be 2.30. From this value, from the apparent crystallinity in the CP experiment, and from an ϵ_C assumed to be 3.5, the true crystallinity (based on differences in line position) of 0.76 is deduced.

The defect intensities of each of the spectra given in Figures 2 and 3 are compiled in Table II. These intensities relate to spectra which have been normalized to the same total intensity. Therefore, these intensities are analogous to concentrations and, therefore, they are expressed in terms of concentrations per 1000 backbone carbons appearing in each spectrum. Another perspective on the concentrations appearing in Table II is that these data

Table II
Apparent Fractions (in Units of 10^{-3}) of Defect Carbons in Experimental and Synthesized Spectra[a]

	experiment					
δ,[b] ppm	(90°–5 s)	CP	SL20+CP	DE5+CP	pure crystal	pure noncrystal
11.3	6.95 ± 0.5	0.96 ± 0.25	<0.25	5.54 ± 0.5	<0.25	5.53 ± 0.4
15	4.76 ± 0.4	1.38 ± 0.2	1.08 ± 0.2	2.27 ± 0.4	1.01 ± 0.14	2.38 ± 0.25
115	2.19 ± 0.3	0.91 ± 0.1	0.62 ± 0.1	1.91 ± 0.3	0.56 ± 0.07	1.99 ± 0.2
139	2.50 ± 0.3	0.94 ± 0.1	0.55 ± 0.1	2.03 ± 0.3	0.54 ± 0.07	2.05 ± 0.2

[a] Resonances at 25 and 40 ppm are not included because of substantial integration uncertainties resulting from partial overlap with the backbone resonances. [b] Chemical shift referred to liquid tetramethylsilane.

Table III
Apparent Partitioning of Defects[a]

	phase				
species	crystal	noncrystal	total	from ^{13}C soln data[e]	from GPC
methyl ends[b]	0.77 ± 0.11	0.57 ± 0.07	1.34 ± 0.18	1.19	
vinyl ends[c]	0.42 ± 0.05	0.49 ± 0.05	0.91 ± 0.10	1.01	
ethyl branches[d]	<0.20	1.33 ± 0.10	1.23–1.63	2.65	
methyl + vinyl ends			2.25	2.20	2.35

[a] Based on the assumption of uniform enhancement factors for the defects and backbone resonances within each phase. Values in the table represent the numbers of defect carbons per 1000 carbons in the whole sample. [b] Based on the 15 ppm resonance. [c] Based on both the 115 and 139 ppm resonances. [d] Based on the 11.3 ppm resonance. [e] Based on average values from our results and Randall's results.

have not yet been evaluated for possible differences in ϵ_{NC}^{d} values compared with ϵ_{NC}. This will be done presently.

In Figure 3, the qualitative conclusions deduced from Figure 2 are borne out, namely, that the concentration of all defects is greater in the noncrystalline region, and, in particular, there is no convincing evidence for the presence of ethyl branches in the crystal. A few points about Table II should be noted. The intensity for the 11.3 ppm resonance in the "pure crystal" spectrum is judged to be less than 0.25 per 1000 backbone carbons. Expressed as concentration then, the ethyl branches appear to be at least 20 times more concentrated in the noncrystalline phase. In terms of the partitioning of end groups, Table II also indicates that vinyls are different from end methyls in that the ratios of apparent noncrystal to crystal concentrations are 2.4 and 3.7, respectively, for the end methyls and the terminal vinyls.

We turn now to the consideration of the defect intensities given in Table II and whether these intensities are consistent with the concentration of defects determined by high-resolution ^{13}C NMR. The origin of this concern is that ϵ_{NC}^{d} values are determined by both $T_{1\rho}^{H}$ and T_{CH}. Although $T_{1\rho}^{H}$ influences are postulated to be quite uniform for both defect and backbone carbons, T_{CH} values need not be since very local motion is important in determining T_{CH}. One might hope that $T_{1\rho}^{H}$ values were the dominant influence at both the defect and backbone carbons with the result that $\epsilon_{NC}^{d} = \epsilon_{NC}$. Then the values given in Table II, when coupled with the actual crystallinity, should reproduce the known total defect concentration. This hypothesis is tested in Table III, where the total number of chain ends and branches in each phase is calculated by multiplying the appropriate defect concentration by the mass fraction of that phase. Also given are the total defect concentrations, and these values are compared with the ^{13}C solution results and the GPC-determined concentration. For the end methyl and the vinyl groups, agreement is reasonably good (10–15% variations). More particularly, the total end-group count agrees within 5% with both of the end-group counts obtained by the other methods. Therefore, for the chain ends, it appears that no further corrections to the intensities need be made. The implication is that approximately 57% of the methyl ends are in crystalline environments whereas only about 46% of vinyl ends are in the crystal.

From Table III, however, a more confusing picture emerges relative to the ethyl branches. Only 46–61% of the total ethyl methyls are accounted for. The problem is that this deficiency may be due to ϵ_{NC}^{d} for the ethyl methyl carbon being about half of ϵ_{NC} for the backbone carbons. Alternatively, and insidiously, it is possible that up to half of the ethyl branches are in the crystal and that the crystalline environment produces a constraint on the branches in such a way that molecular motions in the mid-kilohertz range prevail. In such a case, a strong line broadening[15] could develop for these carbons, which would make them very difficult to see.

Two arguments from the data presented here reduce the plausibility of the latter argument. First, in Figure 3, no methine resonance is visible at 40 ppm corresponding to the branch carbon. The line-broadening mechanism is very local in nature and it is not readily apparent that the methine carbon should be broadened severely if the methyl carbon is broadened. Secondly, the (90°–5 s) experiment provides a second way of checking on the total *observable* ethyl methyl signal. From Table II, the integral of the signal is 6.95×10^{-3}. From Table I, the (90°–5 s) experiment consists of a 72% contribution from the noncrystalline region. Thus since the total ethyl methyl intensity, corresponding to the entire Boltzmann population of observable ethyl methyls appears in the (90°–5 s) experiment, the concentration of observable methyls is $f_{NC} \times (6.95 \times 10^{-3}/0.72) = 2.32 \times 10^{-3}$, where f_{NC} is the true noncrystalline fraction. From this we conclude that at least 87% of the ethyl methyls give observable resonances. Therefore, it follows that no more than 13% of the total branch concentration is invisible by reason of line broadening. It is clear that ethyl branches are largely rejected by the crystal, but the exact number is difficult to determine from these data. At this point, the most likely explanation for the deficiency of total ethyl methyl branch intensity is that the ethyl methyl carbons have a longer T_{CH} than the noncrystalline backbone carbons. We are currently working with a polymer having a higher concentration of ethyl branches in order to answer the question of ethyl branch partitioning more completely. In the extreme case, the 13% invisible ethyl branches are in the crystal along with the 0.2×10^{-3} (threshold) concentration (see Table III), yielding a possible maximum of 20% of the ethyl branches in the crystal.

V. Discussion

The partitioning of the vinyl ends determined in this study stands in considerable contrast to the studies on the accessibility of terminal vinyls to chemical reactants like ozone in a dried single-crystal preparation of PE[20,21] or bromine in a single-crystal liquid suspension.[22,23] Respectively, these studies indicated that 85% and 98% of the vinyls reacted over very short time periods, implying that terminal vinyls were principally rejected by the crystal. In this study we find that only 54% are rejected by the crystal during melt crystallization. The reason for this difference is not apparent although crystallization in dilute solution is certainly a more orderly process from the viewpoint of chain entanglements. Moreover, because the E/B sample has a substantial polydispersity, one would think it reasonable that during slow cooling a molecular weight fractionation was also taking place. If the result of fractionation during crystallization is that the lower molecular weight material (with higher concentrations of chain ends) is preferentially found in the noncrystalline region, then for a PE sample of low polydispersity even a larger fraction of vinyl ends would be incorporated into the crystalline region.

The incorporation of saturated chain ends into the crystalline regions is a subject on which we could find no literature. The result presented here that 57% of the methyls are in the crystalline region does not seem too surprising from the strictly energetic point of view since the methyl group does not distort the neighboring crystalline chains.

The level of incorporation of side branches in the PE crystal is very controversial in the literature. Although there is a consensus that methyl branches should be easily incorporated,[27,36-39] different points of view surround the question of the inclusion of longer branches. Some authors argue that, under equilibrium conditions, longer branches should be totally excluded.[27,36,40] Others argue that melt crystallization is kinetically controlled, resulting in some side-branch incorporation.[41]

Experimentally the principal evidence for crystalline side-branch populations has been a corresponding unit cell expansion, via an increase of the a and b axes, although other factors may influence this expansion.[27,36] By noting that a given concentration of ethyl and methyl branches results in the same lattice expansion, which, in turn, is a greater expansion than found for the same concentrations of longer (up to ten carbons)[42,43] branches, it has been argued[38,39] that both ethyl and methyl branches are incorporated into the crystal in reasonable numbers, while longer branches tend to be excluded. With respect to ethyl and methyl branches, a similar unit cell expansion need not imply the same level of incorporation in the crystal. In fact, a study in progress in our laboratory on a PE with methyl branches indicates a significant level of incorporation of these branches in the crystal, in contrast to what is reported herein for the ethyl branches.

On the other hand, it is known that the effect of branching distribution, e.g., random or blocklike, influences the ability of the crystalline regions to reject defects.[44] Although we do not know the detailed distribution of butene monomer in this particular sample, the number of branches isolated by at least one ethylene monomer on each side is expected to be very close to the number predicted by random addition.[45] Experiments are now under way on a sample of hydrogenated polybutadiene with somewhat different branching distribution and higher concentration of ethyl branches.

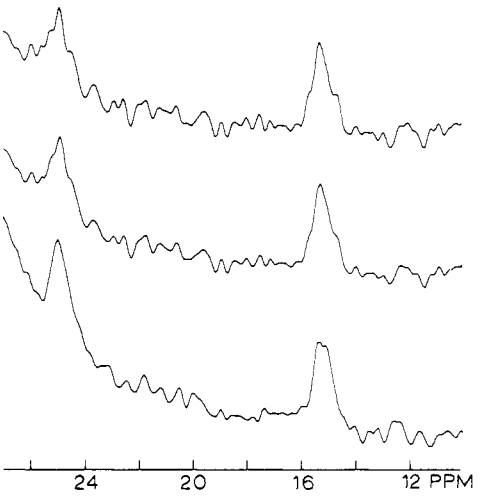

Figure 4. Expanded high-field region of the three candidate "pure crystalline" spectra which were summed to obtain the lower spectrum of Figure 3. These spectra are all normalized to the same total intensity, including the backbone resonances. From top to bottom the spectra represent, respectively, the renormalized linear combinations of the following pairs of CP spectra: (SL20+CP, CP), (SL20+CP, DE5+CP), and (CP, DE5+CP). The similarity of intensities for each of the end-group resonances is taken as evidence for the uniformity of the distribution of defects within the crystalline phase.

Of the assumption invoked in interpreting these experiments, the weakest and least-founded assumption is that of a uniform distribution of defects within each of the two phases. Of course this assumption is tied very closely to the assumption that PE is represented as a two-phase system. Indeed, these phases cannot be uniform; there must be an interface region. And in this region the transition from crystalline order to noncrystalline disorder must be effected. One should consider the influence of this transition zone and whether it is possible that the defects attributed to the crystal are really concentrated in that zone. What follows are a few thoughts and speculations on this possibility.

The first speculation concerns the spectral expression of interface carbon resonances. It is well-known that the shifted resonances, which are defined as noncrystalline in this paper, all have T_1^C values less than 0.5 s and so imply a reasonable mobility. The resonance position, in shifting upfield from the all-trans crystalline resonance, *may* also imply more gauche content in the average conformation of each carbon. On the other hand, what is called crystalline in this study is that which resonates at 32.9 ppm. These latter carbons are not motionally rigid in a uniform sense, a fact recognized by others.[46] There are even nontrivial fractions of this line whose T_1^C values are of the order of a few seconds or tens of seconds. Therefore, those chain segments called crystalline are certainly not uniformly rigid and may include contributions from the constrained crystalline interface. It *may* also be that what is called crystalline in this study are those chain segments whose time-averaged conformation is, for the most part, trans. Since such regions of higher mobility exist, it might follow that these regions could accommodate defects more readily.

This is a difficult possibility to contend with. However, there is some evidence to suggest that defects are not concentrated at the crystalline interface. First, there is a difference of 0.3–0.4 ppm between the resonance maxima of the end methyls in the two spectra of Figure 3. This shows a distinction (although rather small) between the two resonances identified by this decomposition method. However, the crystalline interface may be sufficiently

different from the noncrystalline region to produce such a shift; therefore, this argument is weak.

A second stronger argument relates to the self-consistency of the crystalline spectra obtained via the linear combinations of the spectra in Figure 2. Figure 4 shows an expanded portion of the end-methyl and corresponding α-methylene regions for each of the renormalized linear combinations of the original spectra. (The noncrystalline spectra are individually too noisy to allow one to make the same arguments.) Although the upper two spectra are dominated by the SL20+CP spectrum, the lower spectrum is dominated by the CP spectrum. In terms of the total intensity of each defect resonance, there is good agreement among all of the spectra. Moreover, all of them also agree in showing a lack of ethyl methyl intensity. The question is whether this agreement says anything about a concentrated layer of defects at the crystal interface. This argument may be significant for the reason that the SL20+CP experiment, in contrast to the CP experiment, is biased to suppress crystalline contributions at the interface because proton spin diffusion to the adjacent noncrystalline region is preferentially depleting the polarization of the interface protons relative to the protons in the crystalline core. Therefore, if the defects were concentrated at the crystalline interface one would expect the crystalline contribution to the defect intensity in the SL20+CP to be significantly lower than in the CP experiment. A spectral bias is also possible in the DE5+CP experiment because the crystalline contribution to this spectrum could be interface-rich and thus add an anomalously large contribution from crystalline (really interface) defects. The reason for such a bias developing is that the T_2^H of these more mobile interface protons could be longer than for the rigid crystalline material. Also, proton spin diffusion from the noncrystalline chains could partially polarize some of the interface protons during the 1-ms CP period.

It is hard to quantify the effects of an interface-rich branch distribution on the spectra of Figure 4. It is easy to show that resulting spectral biases lead to "pure crystalline" spectra in which the defect contribution from the crystal, including the crystalline interface, is *underestimated*. Whether the linear combination spectra of Figure 4 would be sensitive to this bias to differing degrees is more difficult to say. Therefore, we only offer Figure 4 as possible further evidence that the defects are evenly distributed throughout the crystalline phase.

The method for generating the "pure" spectra of Figure 3 has not been optimized for signal-to-noise nor for best weighting of the component spectra. It simply represents an approach which did not show obvious experimental favoritism toward any one of the three contributing spectra. In reality, however, a closer look reveals that the SL20+CP spectrum is the strongest contributor to the pure crystalline spectrum, whereas, oddly enough, the CP and SL20+CP spectra are the strongest contributors (contributions of opposite sign) to the pure noncrystalline spectrum. Although it is not shown, a synthesized CP spectrum, generated by mixing the appropriate relative amounts (see Table I) of the spectra in Figure 3, matches the actual CP spectrum very well, including the defect resonances.

We feel that this method, while lacking final rigorous proof as to its experimental validity, is certainly self-consistent in all the tests we have applied, and thus we feel quite confident that this method gives an accurate representation of the true situations so long as total intensities are accounted for. In future work we hope to address questions concerning the partitioning of defects as a function of crystallization conditions, kinds of branches, and molecular polydispersity. We are also in the process of applying these techniques to γ-irradiated samples.

VI. Conclusion

A ^{13}C solid-state NMR method based on a two-phase model for polyethylene and an assumption about the local uniformity of proton spin polarization is shown to lead to a simultaneous separation of both backbone and defect (end group and side branch) resonances into their respective "pure crystalline" and "pure noncrystalline" component spectra. The raw data from which these latter spectra are generated consist of cross-polarization (CP) spectra involving different preparations of proton magnetization. From the "pure" spectra, from a separate measurement of crystallinity, and from an independent knowledge of defect concentrations, the partitioning of each defect between the crystalline and noncrystalline regions is deduced. The principal reason that the CP spectra do not themselves constitute enough information to determine partitioning is that CP efficiencies may vary from line to line.

For the slowly cooled, melt-crystallized ethylene–1-butene linear copolymer (2.65 ethyl branches per 1000 backbone carbons and M_n = 12 500) studied herein, the end methyl and terminal vinyl signals are well-behaved. The "pure" spectra indicate that 57% of the methyl ends and 46% of the vinyl ends are located in the crystalline region, the latter being a much higher level than is found in solution-crystallized polyethylene. No direct evidence of ethyl branches is observed in the "pure crystalline" spectrum. However, in view of the sensitivity limitations and the fact that there seems to be some missing ethyl methyl signal, a maximum of 20% of the ethyl branches could be in the crystal. This means that the concentration of ethyl branches in the noncrystalline region is at least 12.5 times higher than in the crystalline region.

Because of the generally weak intensity of the defect resonances, signal-to-noise considerations are important. The threshold for detecting a defect resonance is about 2 carbons in 10 000 backbone carbons after 12–20 h of signal averaging in a normal CP experiment. However, because the DE5+CP experiment yields a significantly less intense signal than the other two CP experiments do and because there is usually much less noncrystalline compared to crystalline material in PE, the signal-to-noise levels in the "pure noncrystalline" spectra are somewhat poorer. It took about 2.5 days to collect the data for this sample; therefore, this method is not advertised for its high sample throughput. For end-group analysis, M_n = 20 000 should be considered to be a practical upper limit.

Finally, the procedure for isolating the "pure" component spectra assumes that the defects are uniformly distributed throughout each of the two phases. The introduction of a crystalline interface containing a high proportion of crystalline defects was considered and the effect of this interface was shown to cause an underestimate of crystalline defect intensity. A couple of experimental observations were cited, each of which was consistent with the notion of a uniform distribution of defects in a two-phase system, but the uniform distribution is not to be considered proven.

Acknowledgment. We thank Dr. J. C. Randall of Phillips Petroleum for his encouragement, for his helpful discussions, and for supplying us with the E/B polymer and its characterization. E. P. acknowledges the Research Council of Spain (CSIC) for providing support during this

work at the National Bureau of Standards.

Registry No. EB (copolymer), 25087-34-7.

References and Notes

(1) Randall, J. C. In *Polymer Characterization by ESR and NMR*; Woodward, A. E., Bovey, F. A., Eds.; American Chemical Society: Washington, DC, 1980; ACS Symp. Ser. No. 142.
(2) Axelson, D. E.; Levy, G. C.; Mandelkern, L. *Macromolecules* **1979**, *12*, 41.
(3) Dorman, D. E.; Otocka, E. P.; Bovey, F. A. *Macromolecules* **1972**, *5*, 574.
(4) Usami, T.; Takayama, S. *Macromolecules* **1984**, *17*, 1756.
(5) Bovey, F. A.; Schilling, F. C.; McCrackin, F. L.; Wagner, H. L. *Macromolecules* **1976**, *9*, 76.
(6) Sarles, L. R.; Cotts, R. M. *Phys. Rev.* **1958**, *111*, 853.
(7) Pines, A.; Gibby, M. G.; Waugh, J. S. *J. Chem. Phys.* **1973**, *59*, 569.
(8) (a) Andrew, E. R. *Prog. Nucl. Magn. Reson. Spectrosc.* **1972**, *8*, 1. (b) Lowe, I. J. *Phys. Rev. Lett.* **1959**, *2*, 285.
(9) Schaefer J.; Stejskal, E. O.; Buchdahl, R. *Macromolecules* **1975**, *8*, 291.
(10) Lippmaa, E.; Alla, M.; Tuherm, T. In *Proceedings XIX Congress Ampere, Heidelberg, 1976*, p 113.
(11) Garroway, A. N.; Moniz, W. B.; Resing, H. A. *Prepr., Div. Org. Coatings Plast. Chem.* **1976**, *36*, 133.
(12) Schaefer, J.; Stejskal, E. O.; Buchdahl, R. *Macromolecules* **1977**, *10*, 384.
(13) Lyerla, J. R. *Comtemporary Topics in Polymer Science*; Shen, M., Ed.; Plenum: New York, 1979; Vol. 3, p 143.
(14) Lippmaa, E. T.; Alla, M. A.; Pehk, T. J.; Engelhardt, G. *J. Am. Chem. Soc.* **1978**, *100*, 1929.
(15) VanderHart, D. L.; Earl, W. L.; Garroway, A. N. *J. Magn. Reson.* **1981**, *44*, 361.
(16) VanderHart, D. L.; Khoury, F. *Polymer* **1984**, *25*, 1589.
(17) Earl, W. L.; VanderHart, D. L. *Macromolecules* **1979**, *12*, 762.
(18) This value is different from the 33.63 value reported earlier (Earl, W. L.; VanderHart, D. L. *J. Magn. Reson.* **1982**, *48*, 35). Recently, we have recognized that the crystalline PE peak is field-dependent (VanderHart, D. L. *J. Chem. Phys.*, in press).
(19) VanderHart, D. L. *J. Magn. Reson.* **1981**, *44*, 117.
(20) Keller, A.; Priest, D. J. *J. Macromol. Sci. Phys.* **1968**, *B2*, 479.
(21) Keller, A.; Priest, D. J. *J. Polym. Sci., Part B* **1970**, *8*, 13.
(22) Witenhafer, D. E.; Koenig, J. L. *J. Polym. Sci., Part A-2* **1969**, *7*, 1279.
(23) Runt, J.; Harrison, I. R. *J. Polym. Sci., Polym. Phys. Ed.* **1978**, *16*, 375.
(24) Möller, M. *Adv. Polym. Sci.* **1985**, *66*, 59.
(25) Ando, I.; Sorita, T.; Yamanobe, T.; Komoto, T. *Makromol. Chem., Rapid Commun.* **1985**, *6*, 349.
(26) Randall, J. C.; Zoepfl, F. J.; Silverman, J. *Radiat. Phys. Chem.* **1983**, *22*, 183.
(27) Alamo, R.; Domszy, R.; Mandelkern, L. *J. Phys. Chem.* **1984**, *88*, 6587.
(28) (a) Bergman, K.; Nawotki, K. *Kolloid-Z. Z. Polym.* **1967**, *219*, 132. (b) Kitamaru, R.; Horii, F. *Adv. Polym. Sci.* **1978**, *26*, 137.
(29) Certain commercial companies are named in order to specify adequately the experimental procedure. This in no way implies endorsement or recommendation by NBS.
(30) Stejskal, E. O.; Schaefer, J. *J. Magn. Reson.* **1975**, *18*, 560.
(31) Ostroff, E. D.; Waugh, J. S. *Phys. Rev. Lett.* **1966**, *16*, 1097.
(32) Powles, J. G.; Mansfield, P. *Phys. Lett.* **1962**, *2*, 58.
(33) Powles, J. G.; Strange, J. H. *Proc. Phys. Soc. London* **1963**, *82*, 6.
(34) Noggle, J. H.; Schirmer, R. E. In *The Nuclear Overhauser Effect*, Academic: New York, 1971.
(35) Axelson, D. E.; Mandelkern, L. In *Carbon-13 NMR in Polymer Science*; Pasika, W. M., Ed.; American Chemical Society: Washington, DC, 1979; ACS Symp. Ser. No. 103.
(36) Richardson, M. J.; Flory, P. J.; Jackson, J. B. *Polymer* **1963**, *4*, 221.
(37) Baker, C. H.; Mandelkern, L. *Polymer* **1966**, *7*, 71.
(38) Preedy, J. E *Br. Polym. J.* **1973**, *5*, 13.
(39) Balta Calleja, F. J.; Hosemann, R. *J. Polym. Sci., Polym. Phys. Ed.* **1980**, *18*, 1159.
(40) Killian, H. G. *Kolloid-Z. Z. Polym.* **1969**, *231*, 534.
(41) Helfand, E.; Lauritzen, J. I. *Macromolecules* **1973**, *6*, 631.
(42) Swan, P. R. *J. Polym. Sci.* **1962**, *56*, 409.
(43) Shirayama, K.; Kita, S.; Watabe, H. *Makromol. Chem.* **1972**, *151*, 97.
(44) Axelson, D. E. *J. Polym. Sci., Polym. Phys. Ed.* **1982**, *20*, 1427.
(45) Hsieh, E. T.; Randall, J. C. *Macromolecules* **1982**, *15*, 353.
(46) Axelson, D. E.; Mandelkern, L.; Popli, R.; Mathieu, P. *J. Polym. Sci., Polym. Phys. Ed.* **1983**, *21*, 2319.

Investigation of the Thermal Degradation of Poly(acrylic acid) and Poly(methacrylic acid) by High-Resolution ^{13}C CP/MAS NMR Spectroscopy

C. A. Fyfe* and M. S. McKinnon

The Guelph–Waterloo Centre for Graduate Work in Chemistry, Department of Chemistry and Biochemistry, University of Guelph, Guelph, Ontario N1G 2W1, Canada.
Received May 22, 1985; Revised Manuscript Received April 4, 1986

ABSTRACT: The structural changes occurring in poly(acrylic acid) and poly(methacrylic acid) when exposed to high temperatures have been investigated by high-resolution ^{13}C solid-state NMR. The initial step in the decomposition of poly(acrylic acid) involves the formation of anhydrides, the majority of which involve six-membered rings. Continued heating results in the loss of hydrogen from the backbone of the polymer. At higher temperatures, a highly aromatic char with phenol functionalities is formed. Poly(methacrylic acid) also forms six-membered cyclic anhydrides but forms a stable structure at lower temperatures. At much higher temperatures substantial degradation occurs, giving rise to an aromatic char that has phenol functionalities as well as methyl and quaternary carbons.

Introduction

The present work employs high-resolution ^{13}C CP/MAS solid-state NMR spectroscopy to analyze the solid products of the thermal degradation of poly(acrylic acid) and poly(methacrylic acid). In these experiments, a combination of cross-polarization[1] (CP) and "magic-angle" spinning[2] (MAS) with high-power proton decoupling is used to give ^{13}C NMR spectra of moderate to good resolution from completely solid materials.[3,4] The spectra yield the isotropic average chemical shifts (for the solid state) and can be used for structural elucidation by employing the chemical shift correlations from solution ^{13}C NMR as reference data. These techniques have found wide application in the study of insoluble and amorphous materials,[5] where information is severely limited by the lack of a good analytical technique, diffraction techniques not being applicable because of the lack of long-range order. It is also possible to determine additional information

0024-9297/86/2219-1909$01.50/0